

Divergent morphological changes within the orbitofrontal cortex in individuals with congenital olfactory sensory loss

Moa G. Peter^{1*}, Gustav Mårtensson², Elbrich M. Postma^{3,4}, Love Engström Nordin^{2,5}, Eric Westman^{2,6},
Sanne Boesveldt³ & Johan N. Lundström^{1,7,8,9*}

ABSTRACT

Individuals with congenital sensory loss experience a total lack of input from the lost sense throughout development. This lack of input has been linked to altered brain morphology, mainly in cerebral areas normally devoted to the processing of the lost sense. In congenital olfactory sensory loss (anosmia), the only consistent morphological finding is a decreased depth of the olfactory sulci, linked to small or absent olfactory bulbs. Here, we aimed to establish whether congenital anosmia leads to more widespread alterations by comparing gray matter volume, cortical thickness, and curvature between 34 individuals with isolated congenital anosmia and 34 matched controls. Individuals with anosmia demonstrated alterations in bilateral olfactory sulci, encompassing decreased sulcus depth, gray matter atrophy, and decreased curvature. They further demonstrated increased gray matter volume and cortical thickness in the medial orbital gyri; regions strongly linked to olfactory processing, sensory integration and value coding. No structural alterations in the primary olfactory (piriform) cortex were, however, demonstrated. Our results replicate and extend previous knowledge with findings of divergent morphological alterations in bilateral orbitofrontal cortex, indicating influences of different plastic processes and suggesting that a lifelong absence of sensory input does not necessarily lead to morphological alterations in primary sensory cortex.

INTRODUCTION

The notion that the human brain is plastic and undergoes morphological as well as functional alterations in response to changes in experienced demands is widely accepted (Buonomano and Merzenich 1998; Lindenberger et al. 2017). One of the more drastic changes in demands on the brain is undoubtedly the loss of a sensory modality, comprising a complete lack of input from the lost sense combined with altered demands on the remaining senses. Indeed, visual sensory loss has

repeatedly been linked to both structural and functional cerebral reorganizations with, often profound, changes in regions normally focused on the processing of the lost sense (Bavelier and Neville 2002; Merabet and Pascual-Leone 2010; for reviews see Frasnelli et al. 2011). In contrast, little is known about the potential plastic effects of complete olfactory sensory loss (anosmia). Whether individuals with lifelong (congenital)

¹ Department of Clinical Neuroscience, Karolinska Institutet, Stockholm, Sweden

² Department of Neurobiology, Care Sciences and Society, Karolinska Institutet, Stockholm, Sweden

³ Division of Human Nutrition and Health, Wageningen University, Wageningen, the Netherlands

⁴ Smell and Taste Centre, Hospital Gelderse Vallei, Ede, the Netherlands

⁵ Department of Diagnostic Medical Physics, Karolinska University Hospital Solna, Stockholm, Sweden

⁶ Department of Neuroimaging, Centre for Neuroimaging Sciences, Institute of Psychiatry, Psychology and Neuroscience, King's College London, London, UK.

⁷ Monell Chemical Senses Center, Philadelphia, Pennsylvania

⁸ Department of Psychology, University of Pennsylvania, Philadelphia

⁹ Stockholm University Brain Imaging Centre, Stockholm University, Stockholm, Sweden

* Corresponding authors: moa.peter@ki.se johan.lundstrom@ki.se

anosmia display cerebral reorganization is yet to be fully determined.

Although the brain exhibits plasticity throughout life, it is strongest early in life when even brief periods of sensory deprivation can make it difficult, if not impossible, to gain normal abilities even if the sensory loss is reversed and normal sensory input established (Wiesel and Hubel 1965; Hyvärinen et al. 1981; Collignon et al. 2015; Guerreiro et al. 2016). Thus, in comparison to individuals who have gone through normal sensory development, individuals with a congenital or very early acquired complete sensory loss would be expected to demonstrate pronounced patterns of cerebral reorganization. In addition to capturing the reorganization during this period of high plasticity, studying individuals with an isolated congenital sensory loss (i.e., a congenital sensory loss not related to additional symptoms) has the advantage of isolating plastic effects of the sensory deprivation. In contrast, individuals with an acquired sensory loss constitute a much more heterogeneous group where variability in the age at which the sense was lost, the duration of the sensory loss, the direct cause of sensory loss in itself (as in the case of traumatic brain injury, which might in itself cause reorganization of the brain), and perceptual abilities before sensory loss likely affects sensory loss-related cerebral reorganization (Noppeney et al. 2005; Voss and Zatorre 2012). Taken together, individuals with congenital sensory loss constitute an excellent model for increasing the understanding of the adaptiveness the human brain possesses.

Congenital visual sensory loss has repeatedly been demonstrated to lead to atrophy in form of decreased gray matter volume in areas within the visual cortex (Ptito et al. 2008; Bridge et al. 2009), well aligned with the patterns of atrophy demonstrated in individuals with an acquired visual sensory loss (Noppeney et al. 2005; Pan et al. 2007). However, the gray matter volume decreases are associated with divergent underlying

morphology: the atrophy in congenital blindness is accompanied by a thickening of the visual cortex (Bridge et al. 2009; Jiang et al. 2009; Park et al. 2009; Hasson et al. 2016), whereas the atrophy in individuals with acquired sensory loss is linked to a cortical thinning or a lack of cortical thickness alterations (Jiang et al. 2009; Park et al. 2009; Voss and Zatorre 2012). Hence, even though overlap in sensory loss-dependent morphological changes is reported for congenital and acquired sensory loss, the underlying mediating mechanisms might be different. Moreover, the fact that divergent underlying morphology may cause similar volumetric results emphasize the importance of not solely relying on one measure of morphological changes.

In contrast to the homogeneous results in the literature on brain morphology in congenital blindness, the only consistent finding in the study of cerebral morphological reorganization in individuals with isolated congenital anosmia (ICA) is the absence, or hypoplasia, of the olfactory bulbs and olfactory tracts, accompanied by a significant decrease in olfactory sulcus depth (Yousem et al. 1996; Abolmaali et al. 2002; Huart et al. 2011). Despite the established link between olfactory ability and the morphology of olfactory cortical structures such as the olfactory bulb, orbitofrontal cortex (OFC), and piriform (commonly referred to as primary olfactory) cortex, generally indicating a positive correlation between volume and ability (Frasnelli et al. 2010; Seubert, Freiherr, Frasnelli, et al. 2013; Hummel et al. 2015), there are, to the best of our knowledge, only two studies that have investigated whether individuals with ICA display cortical alterations beyond the olfactory bulb, tract, and sulcus in a statistical manner: one by Frasnelli and colleagues (2013) and one by Karstensen and colleagues (2018), including 17 and 11 individuals with ICA, respectively. Both studies indicate that individuals with ICA have altered cortical thickness and/or gray matter volume in olfactory processing areas, such as the piriform cortex and

OFC; results that are in agreement with the visual loss literature where changes within cortical areas important for the processing of the lost sensory modality have repeatedly been demonstrated. However, both studies report unilateral alterations located in opposite hemispheres in combination with additional non-overlapping areas. Importantly, the failure of exact replication does not suggest inaccurate results, but indicate that the sample sizes are likely not large enough to gain sufficient statistical power for stable results. This is not a unique problem. Sample sizes in studies of congenital sensory loss, independent of sensory modality explored, are typically small (undoubtedly a consequence of the scarcity of these conditions) and it is uncommon to include more than 20 patients.

In the present study, we aimed to determine whether cortical morphological alterations beyond the olfactory bulb and olfactory sulcus depth are present in individuals with congenital anosmia. Structural magnetic resonance imaging data was collected for 34 individuals with ICA and 34 normosmic controls, carefully matched in terms of age, sex, and education. First, the depths of the olfactory sulci were measured and compared between groups to replicate past studies indicating that a decreased olfactory sulcus depth can serve as an indicator of congenital anosmia. We thereafter determined potential group differences in gray matter volume using voxel-based morphometry (VBM) for voxel-wise comparisons. Finally, to assess possible underlying mechanisms of the VBM results, we determined potential differences in cortical thickness and curvature between individuals with ICA and healthy controls. Based on past findings indicating that both congenital blindness and ICA leads to an increase in cortical thickness and/or gray matter volume within early processing areas of the lost sense, we hypothesized that individuals with ICA would demonstrate an increase in gray matter volume within piriform

cortex and OFC, and that this increase is linked to an increase in cortical thickness.

MATERIALS AND METHODS

Participants

A total of 68 participants were included in the study: 34 individuals with isolated congenital anosmia (ICA, congenital anosmia unrelated to specific genetic disorders, such as Kallmann syndrome) and 34 healthy controls, matched in terms of sex, age, and educational level (Table 1). Inclusion criterion for the ICA group was a lifelong lack of olfactory perception with no known underlying condition causing the anosmia. In addition, 24 out of the 34 individuals with ICA had received a diagnosis from a physician at a previous occasion. Participants were recruited and tested at two different sites: 46 participants (23 ICA) in Stockholm, Sweden, and 22 (11 ICA) in Wageningen, the Netherlands; the matched control was always tested at the same site as the individual with ICA. One individual from the ICA group was removed from analysis after visual inspection of the images due to abnormal anatomy, leaving a final sample of 33 individuals with ICA and 34 controls. All participants provided written informed consent and the study was approved by the ethical review boards in both Sweden and in the Netherlands.

Procedure

Olfactory testing

Olfactory function was assessed with the full Sniffin' Sticks olfactory test (Burghart, Wedel, Germany), a standardized test consisting of three subtests with individual scores: odor detection threshold (T), odor quality discrimination (D), and 4-alternative cued odor quality identification (I), together yielding the combined TDI-score. Olfactory ability was evaluated against normative data from over 9000 individuals (Oleszkiewicz et al. 2019).

Table 1.

Descriptive statistics per experimental group.

	ICA (n = 33)	Control (n = 34)
Age (years)	34.2 (12.9)	34 (12.1)
Female	21	22
Education (years)	14.1 (2.6)	14.1 (1.7)
TDI	10.9 (2.3)	35.4 (3.8)
<i>Threshold</i>	1.2 (0.5)	8.7 (3.2)
<i>Discrimination</i>	4.9 (1.6)	13.5 (1.6)
<i>Identification</i>	4.8 (1.5)	13.4 (1.3)
Left olfactory sulcus depth (mm)	4.9 (3.3) ^a	8.6 (2.3)
Right olfactory sulcus depth (mm)	5.8 (3.6) ^a	8.8 (2.3)

Values presented as mean (standard deviation). ICA = Isolated congenital anosmia, TDI = combined score from the Sniffin' Sticks olfactory sub-tests.

Image acquisition

Imaging data was acquired on two 3T Siemens Magnetom MR scanners (Siemens Healthcare, Erlangen, Germany). At the Swedish site, data was acquired on a Prisma scanner using a 20-channel head coil and in the Netherlands, a Verio scanner with a 32-channel head coil. The scanning sequence protocols were identical at both sites.

T₁-weighted images with whole-brain coverage were acquired using an MP-RAGE sequence (TR = 1900 ms, TI = 900 ms, TE = 2.52 ms, flip angle = 9°, voxel size = 1 mm³, 176 slices, FoV = 256 mm) and T₂-weighted images with whole-brain coverage were acquired using a SPACE sequence (TR = 3200 ms, TE = 405 ms, voxel size = 1 mm³, 224 slices, FoV = 256 mm). Additional functional imaging data, not reported here, were collected after the anatomical images in the same testing session.

Image processing

All images were visually inspected to ensure high image quality with absence of unwanted artifacts before inclusion.

Olfactory sulcus depth

Two independent raters, blind to participant group, measured the depth of the olfactory sulci in the plane of the posterior tangent through the eyeballs,

according to the method proposed by Huart and colleagues (Huart et al. 2011). In short, on the first slice towards the posterior where the eyeballs were no longer seen on the T₂-weighted MR images, a line measuring the depth of the olfactory sulcus was drawn, using the Multi-Image Analysis GUI software (Mango; <http://ric.uthscsa.edu/mango>). There was a high agreement between the two raters' measurements (intraclass correlation coefficient of .88). Sulci defined as outliers (sulci for which the two initial raters' measurements differed more than 2 standard deviations from the mean difference; in total one sulcus in three individuals and both sulci in three individuals) were assessed by an additional observer. Olfactory sulcus depth was defined as the obtained mean measure, independent of the number of raters.

Volumetric measures

Voxel-based morphometry (VBM, Ashburner and Friston 2000) analysis was done using SPM12 (Wellcome Trust Centre for Neuroimaging, UCL; <http://www.fil.ion.ucl.ac.uk/spm>) in MATLAB 2016a (The MathWorks, Inc., Natick, Massachusetts, USA). T₁-weighted images were segmented into gray matter, white matter, and cerebrospinal fluid in native space using unified segmentation (Ashburner and Friston 2005). The three tissues were used to compute total intracranial

volume for each participant. The gray and white matter were further used as input to a diffeomorphic image registration algorithm to improve inter-subject alignment (DARTEL, Ashburner 2007). DARTEL implements an iterative process in which gray and white matter from all subjects are aligned, creating an increasingly accurate average template for inter-subject alignment. The template and individual flow fields from DARTEL were then used to spatially normalize gray matter images to MNI space with 12 parameter affine transformations. The normalized gray matter images were modulated with the Jacobian determinant of the deformation fields and smoothed (6 mm full-width at half maximum isotropic Gaussian kernel).

Surface based measures

Surface based measures were used to calculate cortical thickness and underlying white matter curvature. The T₁-weighted images were processed using FreeSurfer ver. 6.0 (Dale et al. 1999); <http://surfer.nmr.mgh.harvard.edu/>). The processing pipeline is described in detail elsewhere (Fischl and Dale 2000), but, in short, the image processing included removal of non-brain tissue, Talairach transformation, segmentation of subcortical white matter and gray matter, intensity normalization, tessellation of the boundary between gray and white matter, automated topology correction, and surface deformation to find the gray/white matter boundary and the gray matter/ cerebrospinal fluid boundary. Cortical thickness and mean curvature of the gray/white matter boundary was calculated at each vertex point on the tessellated surface in native space. Thereafter, individual surfaces were aligned to an average template and smoothed (5 mm full-width at half maximum surface based Gaussian kernel) to enable statistical comparisons between the subject groups. FreeSurfer data was pre-processed through the HiveDB database system (Muehlboeck et al. 2014).

Statistical analysis

Olfactory sulcus depth

To assess differences between the two groups in olfactory sulcus depth, a repeated measures analysis of variance (rmANOVA; within subject factor Hemisphere, between subject factor Group) was used with Greenhouse-Geisser correction of degrees of freedom, if the assumption of sphericity was violated according to Mauchly's test; effect size estimates are reported as partial eta-squared (η_p^2). Potential group differences in olfactory sulcus depth were thereafter investigated for the right and left olfactory sulcus separately using Welch's *t*-test. Effects size estimates are given by Cohen's *d*.

Volumetric measures

To compensate for individual differences in intracranial volume when comparing gray matter volume between groups, the pre-processed, normalized gray matter images were proportionally scaled with total intracranial volume. Furthermore, the images were masked with a threshold of 0.15 to avoid inclusion of non-gray matter voxels. Voxel-wise differences in gray matter volume between groups were estimated with independent sample *t*-tests with age, sex, and scanning site as covariates. The tests were corrected for multiple comparisons in a whole-brain analysis with a family-wise error (FWE) corrected significance level of $p < .05$.

Surface based measures

To investigate whether potential volumetric differences can be explained by differences in cortical thickness or curvature, vertex-wise values were compared between groups with age, sex, and scanning site as covariates. Group differences were defined as significant based on a false discovery rate (FDR) of $< .05$. If no vertex survived this threshold, a more liberal threshold of $p < .001$, uncorrected, was used to explore the full extent of potential differences; highlighted in text when used.

RESULTS

Olfactory testing

Mean TDI scores on the Sniffin' Stick olfactory performance test were 10.9 (SD = 2.3, range: 7-15) and 35.4 (SD = 3.8, range: 28.5-42.5) for ICA and controls, respectively (Table 1), with all individuals in the ICA group demonstrating olfactory scores below the limit for functional anosmia (TDI cut-off at 16.0).

Decreased olfactory sulcus depth in individuals with congenital anosmia

Potential differences between individuals with ICA and healthy controls in olfactory sulcus depth were investigated with a rmANOVA. Individuals with ICA demonstrated significantly more shallow olfactory sulci as compared to controls, main effect of Group: $F(1,65) = 23.7, p < .001, \eta_p^2 = .267$; ICA mean = 5.3 mm, SD = 3.4 mm; Control mean = 8.7 mm, SD = 2.3 mm. Furthermore, a difference of depth in the right, as compared to left, olfactory sulcus was demonstrated, main effect of Hemisphere: $F(1,65) = 9.0, p = .004, \eta_p^2 = .122$; however, no significant interaction between Group and Side was present, $F(1,65) = 2.8, p = .09, \eta_p^2 = .042$. The decrease in olfactory sulcus depth for the ICA group was demonstrated for the left olfactory sulcus, $t(57.6) = 5.28, p < .0001, d = 1.3$, as well as for the right olfactory sulcus, $t(54.3) = 4.11, p < .001, d = 1.01$; Figure 1 and Table 1.

Altered morphology within the orbitofrontal cortex in individuals with congenital anosmia

To explore volumetric alterations, voxel-wise tests of group differences in gray matter volume were performed in a VBM analysis. Five clusters passed the FWE-corrected significance level of $p < .05$. All of the significant clusters were located in the orbitofrontal cortex (OFC): two demonstrating gray matter atrophy in the ICA group around the bilateral olfactory sulci, and three clusters demonstrating a gray matter volume increase in the ICA group centered around the bilateral medial orbital gyri; the latter located anterolateral to the

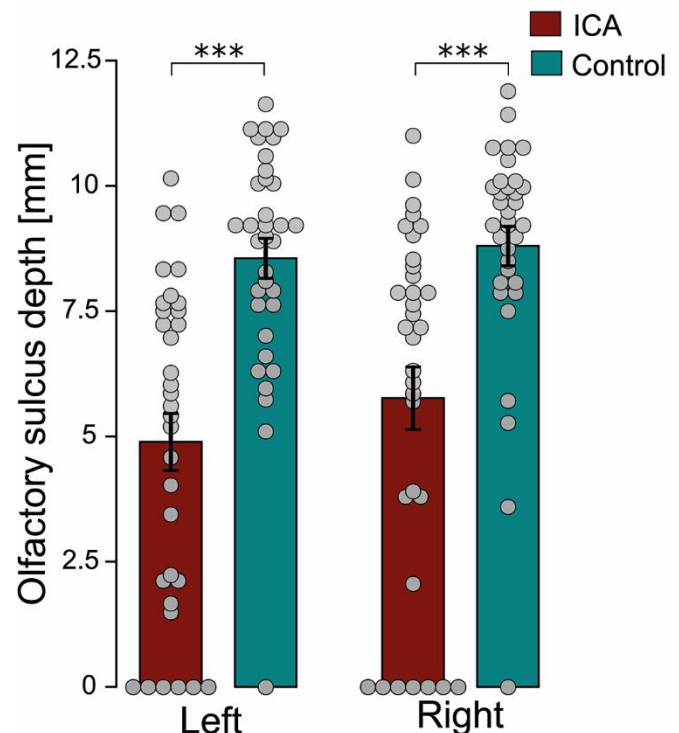


Figure 1 - Group differences in olfactory sulcus depth. Mean olfactory sulcus depth (error bars indicate standard error) overlaid with individual values and separated by hemisphere and group. Individuals with Isolated Congenital Anosmia (ICA) demonstrate a significant decrease in bilateral olfactory sulci compared to matched controls. *** indicating $p < .001$

aforementioned two clusters of gray matter atrophy (Figure 2, Table 2).

In opposition to part of our initial hypothesis, no significant group differences in gray matter volume within piriform cortex (an area often referred to as primary olfactory cortex) were demonstrated at an FWE-corrected significance level of $p < .05$. To confirm that these results were not simply an effect of an excessively conservative statistical threshold, the significance level was altered to $p < .01$, uncorrected. Even at this liberal statistical threshold, no significant group differences in either left or right piriform cortex could be detected (Supplementary Figure S1).

To investigate whether the gray matter volume alterations demonstrated within the ICA group could be further explained by alterations in either cortical thickness or curvature, these measures were compared vertex-wise between groups. The cortical thickness analysis demonstrated a

Table 2.

Results from volumetric measures.

Region	Hemisphere	x ^a	y ^a	z ^a	Cluster size ^b	t ^c	p ^d
<i>ICA < Control</i>							
OFC, olfactory sulcus ¹	L	-12	21	-16	2185	10.5	< .001
OFC, olfactory sulcus ²	R	13	19	-13	2135	9.7	< .001
<i>ICA > Control</i>							
OFC, medial/intermediate orbital gyru	L	-21	39	-21	532	6.7	.001
OFC, medial/intermediate orbital gyrus ⁴	R	17	39	-14	244	6.0	.006
OFC, lateral orbital gyrus	R	22	24	-11	8	5.5	.04

ICA – isolated congenital anosmia, OFC – orbitofrontal cortex. ¹⁻⁴ Clusters used in correlation analysis presented in Table 4. ^a Coordinates derived from MNI152. ^b Cluster size has unit mm³. ^c t-value for peak voxel in cluster ^d p-value for peak voxel, FWE-corrected.

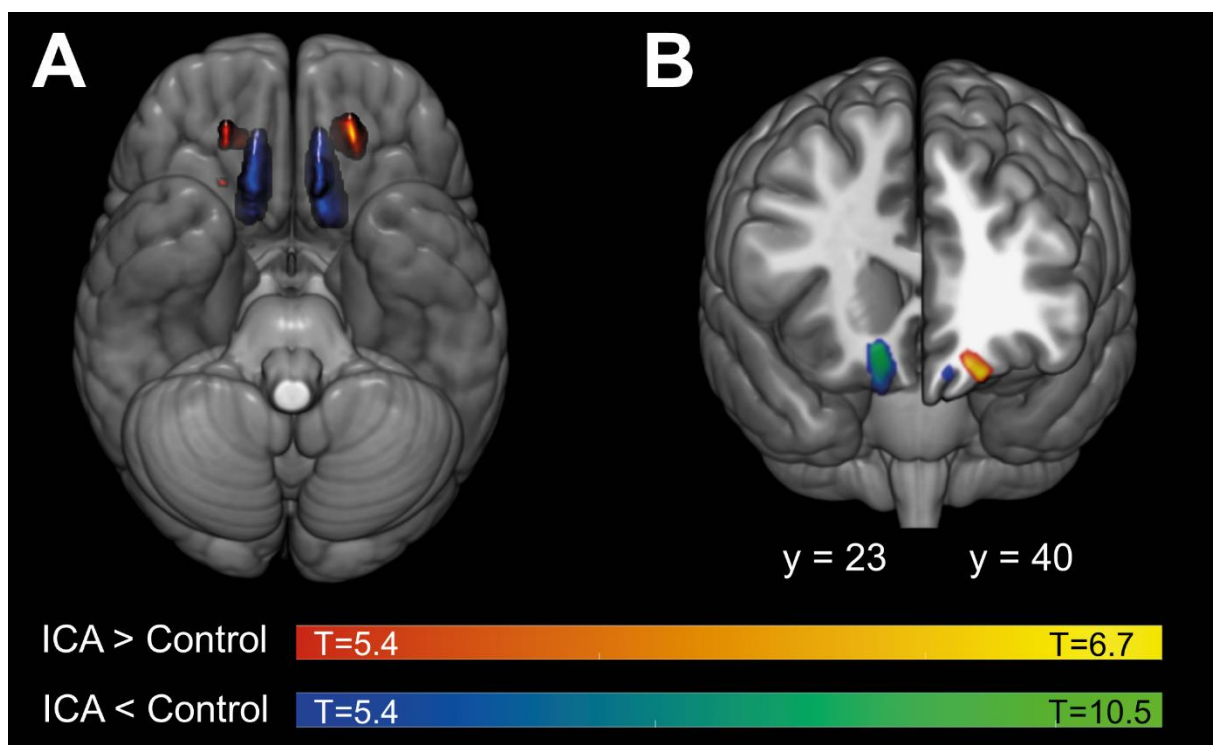


Figure 2 Groups differences in gray matter volume. Gray matter volume differences displayed on MNI152-template. Individuals with isolated congenital anosmia (ICA) demonstrate gray matter volume atrophy in the bilateral olfactory sulci as well as gray matter volume increases in bilateral medial/intermediate orbital gyri. **A** Results displayed on an inferior view of a transparent brain to reveal full extent of clusters. **B** Results displayed on an anterior view with coronal section at y=23 (right hemisphere) and y=40 (left hemisphere). Displayed results are all significant at the level of $p < .05$, FWE-corrected.

thickening of the left middle orbital gyru and anterior olfactory sulcus in the ICA group (Figure 3A, Table 3); however, no group differences in cortical thickness were found in the right hemisphere when using the designated statistical cut-off ($FDR < .05$). When applying a more liberal threshold ($p < .001$, uncorrected), clusters similar

to the ones in the left hemisphere were revealed in the right hemisphere; i.e., cortical thickening around the olfactory sulcus in the ICA group (Figure 3A). In addition to altered gray matter volume and cortical thickness in the OFC, the ICA group further demonstrated decreased curvature around the same orbitofrontal areas: the bilateral

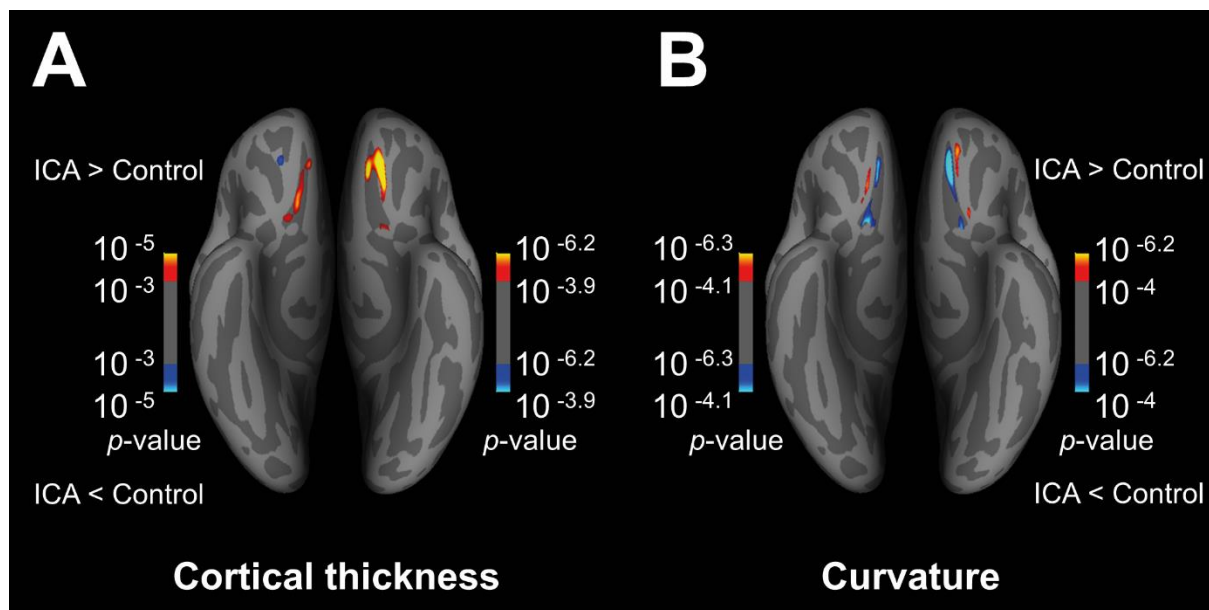


Figure 3 - Group differences in surface based measures. Results are displayed on inflated brain, inferior view. **A** Differences in cortical thickness with warm colors indicating cortical thickness increases in individuals with Isolated Congenital Anosmia (ICA) as compared to normosmic controls. Individuals with ICA demonstrate a significant increase in cortical thickness in the medial orbital gyrus/olfactory sulcus. On the left hemisphere, p-values are thresholded at FDR < .05. No significant group differences were demonstrated in the right hemisphere at this statistical threshold and the clusters in the right hemisphere are therefore thresholded at $p < .001$ uncorrected for visual comparison. **B** Group differences in curvature. Significant differences demonstrated in bilateral olfactory sulcus and bilateral medial orbital gyrus; all indicating a lower absolute value of curvature for individuals with ICA, i.e., larger radii of curves (FreeSurfer's convention of curvature is negative for gyri and positive for sulci, warm colors indicate ICA > Control). Both hemispheres thresholded at FDR < .05.

Table 3.

Results from surface based measures.

Region	Hemisphere	x ^a	y ^a	z ^a	Cluster size ^b	p ^c
Cortical Thickness						
<i>ICA > Control</i>						
OFC, medial orbital gyrus ⁵	L	-15	35	-22	171	10 ⁻¹⁰
OFC, posterior orbital gyrus	L	-16	8	-16	12	10 ^{-4.4}
Curvature						
<i>ICA < Control</i>						
OFC, olfactory sulcus ⁶	L	-12	37	-20	77	10 ⁻¹²
OFC, medial orbital gyrus ⁷	L	-14	42	-22	35	10 ^{-5.9}
Superior temporal sulcus	L	-55	-43	7	22	10 ^{-4.7}
OFC, olfactory sulcus ⁸	L	-16	10	-16	16	10 ^{-5.8}
OFC, medial/posterior orbital gyrus	L	-17	15	-22	9	10 ^{-5.2}
OFC, olfactory sulcus ⁹	R	16	10	-15	56	10 ^{-6.6}
OFC, olfactory sulcus ¹⁰	R	15	33	-19	34	10 ^{-6.3}
OFC, medial orbital gyrus ¹¹	R	14	25	-25	15	10 ^{-5.6}
OFC, medial/ posterior orbital gyrus	R	16	17	-23	2	10 ^{-4.2}

ICA – isolated congenital anosmia, OFC – orbitofrontal cortex. ⁵⁻¹¹ Clusters used in correlation analysis presented in Table 4. ^a

Coordinates derived from MNI305. ^b Cluster size has unit mm². ^c p-value for peak vertex in cluster, uncorrected but surviving FDR < .05.

^d ICA < Control indicates that individuals with anosmia has a lower *absolute* curvature, i.e., a higher radius of curvature. FreeSurfer's convention of curvature is negative for gyri and positive for sulci, which means some of these contrasts are positive and some negative (see Figure 3B).

olfactory sulci and medial orbital gyri, at an FDR threshold of < .05 in the left as well as the right hemisphere (Figure 3B, Table 3). Furthermore, a small cluster of increased curvature was demonstrated in the left superior temporal sulcus (Table 3, Supplementary Figure S2).

Correlation analysis

Both volumetric and surface based analysis revealed structural group differences in bilateral medial OFC, in, or in close proximity to, the olfactory sulci. Based on these results, we assessed whether the volumetric and surface based group differences were linked to group difference in olfactory sulcus depth by means of Pearson's correlation coefficient analyses. For each individual, mean gray matter volume was computed for each of the four large significant clusters. Similarly, mean cortical thickness was computed for the large significant cluster in the left hemisphere, and mean curvature was computed in the three largest significant cluster in left OFC and the three largest significant clusters in right OFC (all clusters used for correlation analysis marked in Table 2 and Table 3). Pearson's correlation

coefficient was computed between each of these structural measures and the olfactory sulcus depth in the corresponding hemisphere, with Bonferroni correction applied for number of tests of each type of structural measure (4 for volume, 6 for curvature). To avoid that the large demonstrated differences between groups would influence the correlations, the Pearson's correlation coefficients were computed within each group separately.

For the volumetric measures, the only significant correlation was between the gray matter cluster around the right olfactory sulcus and the olfactory sulcus depth in the ICA, but not control group (Table 4). Both the ICA and control groups demonstrated significant negative correlation between olfactory sulcus depth and cortical thickness, as well as between olfactory sulcus depth and curvature, in the left medial orbital gyrus. Furthermore, the curvature in the neighboring cluster in the left anterior olfactory sulcus correlated with olfactory sulcus depth in the control (but not ICA) group, whereas corresponding cluster in the right hemisphere

Table 4.

Correlations between listed clusters and olfactory sulcus depth in corresponding hemisphere

Region	Hemisphere	ICA		Control	
		<i>r</i>	<i>p</i>	<i>r</i>	<i>p</i>
VBM					
OFC, olfactory sulcus ¹	L	.06	.746	-.29	.097
OFC, olfactory sulcus ²	R	.59	.002 **	.25	.16
OFC, medial/intermediate orbital gyrus ³	L	.12	.491	-.24	.166
OFC, medial/intermediate orbital gyrus ⁴	R	.31	.077	.25	.148
Cortical thickness					
OFC, medial orbital gyrus ⁵	L	-.51	.003 **	-.59	2.7·10 ⁻⁴ ***
Curvature					
OFC, olfactory sulcus ⁶	L	.24	.172	.50	.003 *
OFC, medial orbital gyrus ⁷	L	-.5	.003 *	-.63	6.3·10 ⁻⁵ ***
OFC, olfactory sulcus ⁸	L	.3	.087	.24	.168
OFC, olfactory sulcus ⁹	R	.24	.187	-.08	.654
OFC, olfactory sulcus ¹⁰	R	.57	.001 **	.13	.454
OFC, medial orbital gyrus ¹¹	R	-.27	.134	-.02	.892

ICA – isolated congenital anosmia, OFC – orbitofrontal cortex, *r* – Person correlation coefficient, asterisks mark Bonferroni corrected significance levels corresponding to * *p* < .05, ** *p* < .01, *** *p* < .001. ¹⁻¹¹ cluster numbers corresponding to the ones in Table 2 and Table 3.

(anterior olfactory sulcus) correlated with olfactory sulcus depth in the ICA group.

DISCUSSION

We can here demonstrate that individuals with isolated congenital anosmia (ICA) have a significantly altered structure in the bilateral medial orbitofrontal cortex (OFC), a multimodal region with a crucial role in olfactory processing. Specifically, individuals with ICA demonstrated structural alterations, compared to normosmic individuals, in and around the olfactory sulci, encompassing a decrease in olfactory sulcus depth and curvature. This was further accompanied by gray matter volume atrophy in the olfactory sulci stretching towards the medial orbital gyri. Moreover, gray matter volume and cortical thickness increases were demonstrated in the medial orbital gyri of individuals with ICA. These divergent results in neighboring cortical areas indicate that the cerebral plasticity caused by a life-long olfactory sensory deprivation cannot be explained by a simple morphological mechanism applied to all olfactory-related cerebral areas, but rather, that the plasticity is area- or network-dependent.

Our results demonstrate that the OFC of individuals with ICA has a distinctly different structure than that of normosmic individuals. Although it is evident that this cortical reorganization is strongly related to the congenital sensory loss, the presented results are in their nature insufficient to conclude how these anomalies emerged. One hypothesis is that individuals with ICA are born with an abnormality in the cortical folding of the medial OFC, manifested as a cortical flattening around the olfactory sulcus and medial orbital gyrus, linked to the absence, or hypoplasia, of the olfactory bulbs and tracts. The olfactory bulbs and tracts reside in the olfactory sulci and the projection of the olfactory tracts is suggested to play an important role in the formation and deepening of the olfactory sulci during early development (Abolmaali et al.

2002; Turetsky et al. 2009; Huart et al. 2011). A congenital abnormal cortical folding explains not only the decreased olfactory sulcus depth and decreased curvature in olfactory sulci and medial orbital gyri, but also the decreased gray matter volume in the olfactory sulci, as a natural consequence of the decreased surface (Karstensen et al. 2018). However, a decrease in cortical surface in the pericalcarine sulci (visual cortex) in congenitally blind individuals has been described by Park and colleagues (Park et al. 2009). This suggests that the decreased olfactory sulcus depth in individuals with ICA might not be exclusively caused by a congenital abnormal anatomy linked to small or absent olfactory bulbs and tracts, but, similar to the blind, be a consequence of atypical development caused by a lack of sensory input. In addition, although the theory of congenital abnormal cortical folding in individuals with ICA provides a straightforward explanation of the decreases in volume and curvature around the olfactory sulci, it cannot fully explain the cortical thickness and gray matter volume increases in the medial orbital gyri. By taking the proposed function of these cortical areas into account, other possible explanations of the cortical reorganization emerge.

The medial OFC is alongside the piriform cortex considered vital for olfactory processing (Gottfried 2006; Lundström et al. 2011; Seubert, Freiherr, Djordjevic, et al. 2013) and the cortical regions in which the individuals with ICA demonstrated cortical thickness and gray matter volume increases show a substantial overlap with areas repeatedly implicated in olfactory processing (Gottfried and Zald 2005; for reviews see Seubert, Freiherr, Djordjevic, et al. 2013). Considering these orbitofrontal areas as predominantly olfactory, the cortical increases displayed by individuals with ICA are presumably caused by the fact that these areas have never received olfactory input. In contrast, individuals with acquired olfactory sensory loss tend to demonstrate cortical volume

decreases in the OFC (Bitter et al. 2010; Yao et al. 2017). Although these morphological consequences of olfactory sensory loss might seem contradictory, similar results have repeatedly been demonstrated in blind individuals, with a thickening of visual cortex of congenitally blind and a thinning of those with acquired blindness (Park et al. 2009; Voss and Zatorre 2012). In addition, the demonstrated cortical volume and thickness increases reported here are an extension of Frasnelli and colleagues' (2013) report of increased cortical thickness in the OFC of individuals with ICA. Cortical increases as a result of a lack of sensory processing might seem counter intuitive and the mechanisms behind these morphological alterations are not yet fully understood. One of the main theories proposed to explain the cortical increases in congenitally blind individuals (Jiang et al. 2009; Park et al. 2009), as well as in individuals with ICA (Frasnelli et al. 2013), is that the complete lack of sensory input to a cortical area normally devoted to the processing of the lost sensory modality alters normal postnatal development. Specifically, the absent input results in a lack of the typical sensory input-driven synaptic pruning of redundant connections. Although the OFC undoubtedly is important for olfactory processing, it is a much more multimodal area than the visual areas showing cortical thickness increases in congenitally blind. Generally, the key functions of the OFC is often put in the context of value encoding, including, but by no means limited to the olfactory domain (Kringelbach and Rolls 2004; Gottfried and Zelano 2011; van den Bosch et al. 2014), with direct stimulation of human OFC eliciting not only olfactory but also somatosensory, gustatory, and emotional experiences (Fox et al. 2018). Specifically, the OFC is relevant for the processing and integration of information from different sensory modalities, receiving olfactory, gustatory, somatosensory, visceral, visual, and auditory input (Ongür and Price 2000; Kringelbach and Rolls 2004; Rolls 2005), and the medial OFC has been

suggested to be of high importance for food consumption (Rolls 2005; Price 2008). If we consider the medial OFC as a multimodal rather than predominantly olfactory processing area, it can be argued that increases in gray matter volume and cortical thickness are not, as previously argued, caused by a lack of synaptic pruning due to absent olfactory input but, to the contrary, related to increased processing of the non-olfactory functions of the OFC. To find support for either theory, the understanding of the specific function of the orbitofrontal areas demonstrating structural reorganization in individuals with ICA needs to be further investigated, preferably using functional neuroimaging methods, to delineate whether the structural reorganization in the individuals with ICA is accompanied by altered function and connectivity.

The cortical structural reorganization demonstrated by individuals with ICA were restricted to higher order olfactory (medial orbitofrontal) cortex, without indications of structural alterations in the primary olfactory (piriform) cortex. This lack of reorganization in primary sensory cortex is in disagreement with the literature on congenital visual sensory loss (Bridge et al. 2009; Jiang et al. 2009; Park et al. 2009; Hasson et al. 2016), as well as previous studies on individuals with congenital anosmia (Frasnelli et al. 2013; Karstensen et al. 2018). Although the two previous studies investigating cortical morphology in individuals with congenital anosmia indicate increased cortical thickness and increased gray matter volume within the piriform cortex, their results are, however, unilateral and in opposite hemispheres. Albeit our results are contradictory to both the aforementioned results and our own hypothesis, the lack of morphological group differences in the piriform cortex reported here are arguably reliable as they are based on considerably larger samples than the two previous studies. In addition, neither volumetric nor surface based measures detected alterations in piriform cortex; measures that did,

however, indicate clear morphological reorganization in medial orbitofrontal areas. It could be argued that ICA does lead to structural alterations in piriform cortex but that the effects are modest, thus limiting the possibility of discovery. Speaking against this argument is the lack of observable differences even when applying a liberal statistical threshold, uncorrected for multiple comparisons. Nonetheless, the piriform cortex is a small structure with complex folding and to firmly establish that a lifelong lack of olfactory perception does not alter its structure, studies with higher spatial resolution should be conducted. Moreover, it should be noted that a lack of morphological changes does not necessarily indicate a lack of functional reorganizations in the piriform cortex due to absent olfactory sensory input.

In addition to the clear reorganization in the orbitofrontal cortex, confirmed with both volumetric and surface based methods, individuals with ICA demonstrated a small but statistically significant cluster of altered curvature in the left superior temporal sulcus. The superior temporal sulcus is, along with the intraparietal sulcus and the prefrontal cortex, one of the classical cortical multisensory integration areas (Ghazanfar and Schroeder 2006; Stein and Stanford 2008; Regenbogen et al. 2017). Although the group difference in the superior temporal sulcus is restricted to the curvature measure, it is noteworthy that a recent study demonstrated that individuals with ICA performed better than normosmic individuals at tasks demanding audio-visual integration; an effect that was interpreted as compensatory abilities due to the sensory loss (Peter et al. 2019). Whether the deviating anatomy in the superior temporal sulcus demonstrated here is related to the compensatory processing of multisensory stimuli in individuals with ICA previously reported should be investigated using functional neuroimaging techniques.

In line with previous studies, we could demonstrate that individuals with ICA have a significantly decreased olfactory sulcus depth, as compared to matched normosmic individuals (Yousem et al. 1996; Abolmaali et al. 2002; Huart et al. 2011; Levy et al. 2013; Karstensen et al. 2018). The shallow olfactory sulcus depth in individuals with ICA is thought to be related to the complete lack of, or hypoplasia of, olfactory bulbs, often accompanied by small or absent olfactory tracts (Yousem et al. 1996; Abolmaali et al. 2002); structures located in the olfactory sulci. Because the olfactory tracts and bulbs can be difficult to image with high quality using standard structural MRI, the olfactory sulcus depth has been suggested to be a valid measure of congenital anosmia, extending or completely replacing the olfactory tracts and bulbs as measures of congenital olfactory sensory loss (Abolmaali et al. 2002; Huart et al. 2011). The measure of olfactory sulcus depth as an indication of congenital rather than acquired olfactory sensory loss is further supported by the fact that a difference in olfactory bulb size, but *not* in olfactory sulcus depth, is found between individuals with acquired anosmia and controls (Rombaux et al. 2010). It is, however, important to note that even though there are significant group differences between individuals with ICA and normosmic individuals, the use of olfactory sulcus depth of a certain value as a tool to diagnose olfactory dysfunction does not allow for an unambiguous diagnose, as there is overlap between groups in sulcus depth. In addition, contrary to the study by Rombaux and colleagues (2010), others have demonstrated a link between the depth of the olfactory sulcus and olfactory abilities in normosmic individuals and in individuals with olfactory loss (Hummel et al. 2003, 2015). Hence, although the literature provides ambiguous results, olfactory sulcus depth has been linked to olfactory abilities beyond individuals with congenital anosmia. What the potential mechanisms mediating the link between olfactory ability and olfactory sulcus depth are, and whether the same

mechanisms apply also for individuals with ICA, still needs to be determined.

The majority of structural differences between individuals with ICA and controls appeared symmetrically in both hemispheres, but the cortical thickness increase in the ICA group was only evident in the left hemisphere when applying the strict criterion of $FDR < .05$. A similar pattern of cortical thickening appeared also in the right hemisphere when applying more liberal statistical threshold. A left-bound lateralization in OFC morphology was also indicated in the study by Karstensen and colleagues (2018), who demonstrated a significant decrease of gray matter volume in the left, but not right, olfactory sulcus of individuals with congenital anosmia. These results could potentially be related to the shallower left olfactory sulcus, a hypothesis consistent with the fact that we could demonstrate a negative correlation between the cortical thickness (as well as the curvature in the left medial orbital gyrus) and the left olfactory sulcus depth. The causes of this modest morphological lateralization and its potential functional implications are yet to be determined.

In conclusion, the current study demonstrates substantial cortical reorganization beyond the olfactory bulb and olfactory sulcus depth in individuals with ICA. The structural alterations are all, except for a small region in the superior temporal sulcus, restricted to the OFC and indicate areas of atrophy as well as increases in individuals born without the olfactory sense. This could potentially be due to a combination of congenital alterations and sensory loss-dependent plastic reorganization occurring during development. These clear findings are based on what we believe is the largest sample of individuals with a congenital sensory loss included in a study statistically comparing gray matter morphology throughout the brain and motivate future studies of the functional relevance of these morphological alterations.

CONFLICT OF INTEREST

The authors have no conflict of interest to report

ACKNOWLEDGEMENTS

This work was supported by the Knut and Alice Wallenberg Foundation (KAW 2018.0152 to J.N.L.) and the Swedish Research Council (2014-1346 to J.N.L.).

REFERENCES

- Abolmaali ND, Hietschold V, Vogl TJ, Hüttenbrink K-B, Hummel T. 2002. MR evaluation in patients with isolated anosmia since birth or early childhood. *AJNR Am J Neuroradiol.* 23:157–164.
- Ashburner J. 2007. A fast diffeomorphic image registration algorithm. *Neuroimage.* 38:95–113.
- Ashburner J, Friston KJ. 2000. Voxel-based morphometry--the methods. *Neuroimage.* 11:805–821.
- Ashburner J, Friston KJ. 2005. Unified segmentation. *Neuroimage.* 26:839–851.
- Bavelier D, Neville HJ. 2002. Cross-modal plasticity: where and how? *Nat Rev Neurosci.* 3:443–452.
- Bitter T, Gudziol H, Burmeister HP, Mentzel H-J, Guntinas-Lichius O, Gaser C. 2010. Anosmia leads to a loss of gray matter in cortical brain areas. *Chem Senses.* 35:407–415.
- Bridge H, Cowey A, Ragge N, Watkins K. 2009. Imaging studies in congenital anophthalmia reveal preservation of brain architecture in “visual” cortex. *Brain.* 132:3467–3480.
- Buonomano DV, Merzenich MM. 1998. Cortical plasticity: from synapses to maps. *Annu Rev Neurosci.* 21:149–186.

- Collignon O, Dormal G, de Heering A, Lepore F, Lewis TL, Maurer D. 2015. Long-Lasting Crossmodal Cortical Reorganization Triggered by Brief Postnatal Visual Deprivation. *Curr Biol.* 25:2379–2383.
- Dale AM, Fischl B, Sereno MI. 1999. Cortical surface-based analysis. I. Segmentation and surface reconstruction. *Neuroimage.* 9:179–194.
- Fischl B, Dale AM. 2000. Measuring the thickness of the human cerebral cortex from magnetic resonance images. *Proc Natl Acad Sci U S A.* 97:11050–11055.
- Fox KCR, Yih J, Raccach O, Pendekanti SL, Limbach LE, Maydan DD, Parvizi J. 2018. Changes in subjective experience elicited by direct stimulation of the human orbitofrontal cortex. *Neurology.*
- Frasnelli J, Collignon O, Voss P, Lepore F. 2011. Crossmodal plasticity in sensory loss. *Prog Brain Res.* 191:233–249.
- Frasnelli J, Fark T, Lehmann J, Gerber J, Hummel T. 2013. Brain structure is changed in congenital anosmia. *Neuroimage.* 83:1074–1080.
- Frasnelli J, Lundström JN, Boyle JA, Djordjevic J, Zatorre RJ, Jones-Gotman M. 2010. Neuroanatomical correlates of olfactory performance. *Exp Brain Res.* 201:1–11.
- Ghazanfar AA, Schroeder CE. 2006. Is neocortex essentially multisensory? *Trends Cogn Sci (Regul Ed).* 10:278–285.
- Gottfried JA. 2006. Smell: central nervous processing. *Adv Otorhinolaryngol.* 63:44–69.
- Gottfried JA, Zald DH. 2005. On the scent of human olfactory orbitofrontal cortex: meta-analysis and comparison to non-human primates. *Brain Res Brain Res Rev.* 50:287–304.
- Gottfried JA, Zelano C. 2011. The value of identity: olfactory notes on orbitofrontal cortex function. *Ann N Y Acad Sci.* 1239:138–148.
- Guerreiro MJS, Putzar L, Röder B. 2016. Persisting Cross-Modal Changes in Sight-Recovery Individuals Modulate Visual Perception. *Curr Biol.* 26:3096–3100.
- Hasson U, Andric M, Atilgan H, Collignon O. 2016. Congenital blindness is associated with large-scale reorganization of anatomical networks. *Neuroimage.* 128:362–372.
- Huart C, Meusel T, Gerber J, Duprez T, Rombaux P, Hummel T. 2011. The depth of the olfactory sulcus is an indicator of congenital anosmia. *AJNR Am J Neuroradiol.* 32:1911–1914.
- Hummel T, Damm M, Vent J, Schmidt M, Theissen P, Larsson M, Klusmann J-P. 2003. Depth of olfactory sulcus and olfactory function. *Brain Res.* 975:85–89.
- Hummel T, Urbig A, Huart C, Duprez T, Rombaux P. 2015. Volume of olfactory bulb and depth of olfactory sulcus in 378 consecutive patients with olfactory loss. *J Neurol.* 262:1046–1051.
- Hyvärinen J, Carlson S, Hyvärinen L. 1981. Early visual deprivation alters modality of neuronal responses in area 19 of monkey cortex. *Neurosci Lett.* 26:239–243.
- Jiang J, Zhu W, Shi F, Liu Y, Li J, Qin W, Li K, Yu C, Jiang T. 2009. Thick visual cortex in the early blind. *J Neurosci.* 29:2205–2211.
- Karstensen HG, Vestergaard M, Baaré WFC, Skimminge A, Djurhuus B, Ellefsen B, Brüggemann N, Klausen C, Leffers A-M, Tommerup N, Siebner HR. 2018. Congenital olfactory impairment is linked to cortical changes in prefrontal and limbic brain regions. *Brain Imaging Behav.* 12:1569–1582.

- Kringelbach ML, Rolls ET. 2004. The functional neuroanatomy of the human orbitofrontal cortex: evidence from neuroimaging and neuropsychology. *Prog Neurobiol.* 72:341–372.
- Levy LM, Degnan AJ, Sethi I, Henkin RI. 2013. Anatomic olfactory structural abnormalities in congenital smell loss: magnetic resonance imaging evaluation of olfactory bulb, groove, sulcal, and hippocampal morphology. *J Comput Assist Tomogr.* 37:650–657.
- Lindenberger U, Wenger E, Lövdén M. 2017. Towards a stronger science of human plasticity. *Nat Rev Neurosci.* 18:261–262.
- Lundström JN, Boesveldt S, Albrecht J. 2011. Central processing of the chemical senses: an overview. *ACS Chem Neurosci.* 2:5–16.
- Merabet LB, Pascual-Leone A. 2010. Neural reorganization following sensory loss: the opportunity of change. *Nat Rev Neurosci.* 11:44–52.
- Muehlboeck J-S, Westman E, Simmons A. 2014. TheHiveDB image data management and analysis framework. *Front Neuroinformatics.* 7:49.
- Noppeney U, Friston KJ, Ashburner J, Frackowiak R, Price CJ. 2005. Early visual deprivation induces structural plasticity in gray and white matter. *Curr Biol.* 15:R488–R490.
- Oleszkiewicz A, Schriever VA, Croy I, Hähner A, Hummel T. 2019. Updated Sniffin' Sticks normative data based on an extended sample of 9139 subjects. *Eur Arch Otorhinolaryngol.* 276:719–728.
- Ongür D, Price JL. 2000. The organization of networks within the orbital and medial prefrontal cortex of rats, monkeys and humans. *Cereb Cortex.* 10:206–219.
- Pan W-J, Wu G, Li C-X, Lin F, Sun J, Lei H. 2007. Progressive atrophy in the optic pathway and visual cortex of early blind Chinese adults: A voxel-based morphometry magnetic resonance imaging study. *Neuroimage.* 37:212–220.
- Park H-J, Lee JD, Kim EY, Park B, Oh M-K, Lee S, Kim J-J. 2009. Morphological alterations in the congenital blind based on the analysis of cortical thickness and surface area. *Neuroimage.* 47:98–106.
- Peter MG, Porada DK, Regenbogen C, Olsson MJ, Lundström JN. 2019. Sensory loss enhances multisensory integration performance. *Cortex.* 120:116–130.
- Price JL. 2008. Multisensory convergence in the orbital and ventrolateral prefrontal cortex. *Chemosens Percept.* 1:103–109.
- Ptito M, Schneider FCG, Paulson OB, Kupers R. 2008. Alterations of the visual pathways in congenital blindness. *Exp Brain Res.* 187:41–49.
- Regenbogen C, Axelsson J, Lasselin J, Porada DK, Sundelin T, Peter MG, Lekander M, Lundström JN, Olsson MJ. 2017. Behavioral and neural correlates to multisensory detection of sick humans. *Proc Natl Acad Sci U S A.* 114:6400–6405.
- Rolls ET. 2005. Taste, olfactory, and food texture processing in the brain, and the control of food intake. *Physiol Behav.* 85:45–56.
- Rombaux P, Potier H, Markessis E, Duprez T, Hummel T. 2010. Olfactory bulb volume and depth of olfactory sulcus in patients with idiopathic olfactory loss. *Eur Arch Otorhinolaryngol.* 267:1551–1556.
- Seubert J, Freiherr J, Djordjevic J, Lundström JN. 2013. Statistical localization of human

- olfactory cortex. *Neuroimage*. 66:333–342.
- Seubert J, Freiherr J, Frasnelli J, Hummel T, Lundström JN. 2013. Orbitofrontal cortex and olfactory bulb volume predict distinct aspects of olfactory performance in healthy subjects. *Cereb Cortex*. 23:2448–2456.
- Stein BE, Stanford TR. 2008. Multisensory integration: current issues from the perspective of the single neuron. *Nat Rev Neurosci*. 9:255–266.
- Turetsky BI, Crutchley P, Walker J, Gur RE, Moberg PJ. 2009. Depth of the olfactory sulcus: a marker of early embryonic disruption in schizophrenia? *Schizophr Res*. 115:8–11.
- Van den Bosch I, Dalenberg JR, Renken R, van Langeveld AWB, Smeets PAM, Griffioen-Roose S, Ter Horst GJ, de Graaf C, Boesveldt S. 2014. To like or not to like: neural substrates of subjective flavor preferences. *Behav Brain Res*. 269:128–137.
- Wiesel TN, Hubel DH. 1965. Extent of recovery from the effects of visual deprivation in kittens. *J Neurophysiol*. 28:1060–1072.
- Voss P, Zatorre RJ. 2012. Occipital cortical thickness predicts performance on pitch and musical tasks in blind individuals. *Cereb Cortex*. 22:2455–2465.
- Yao L, Yi X, Pinto JM, Yuan X, Guo Y, Liu Y, Wei Y. 2017. Olfactory cortex and Olfactory bulb volume alterations in patients with post-infectious Olfactory loss. *Brain Imaging Behav*. 12:1–8.
- Yousem DM, Geckle RJ, Bilker W, McKeown DA, Doty RL. 1996. MR evaluation of patients with congenital hyposmia or anosmia. *AJR Am J Roentgenol*. 166:439–443.